#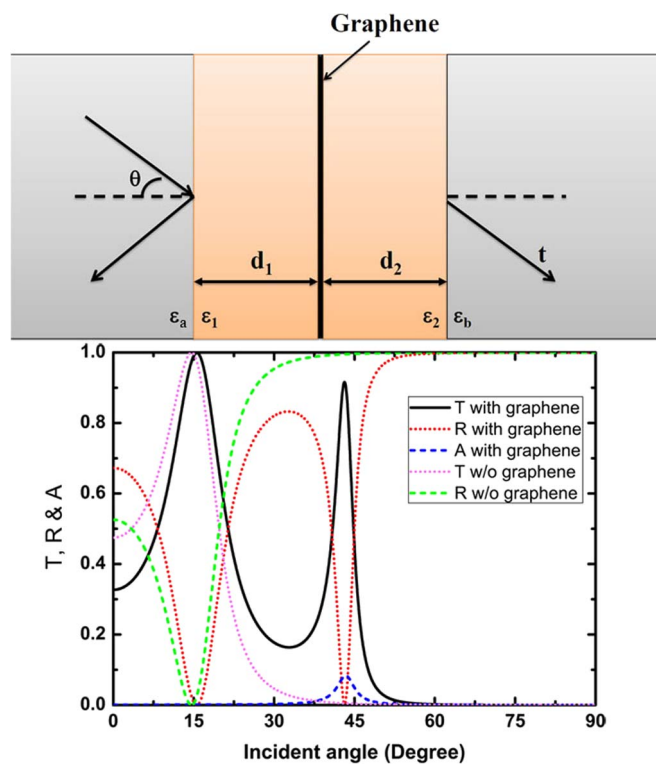 Tunable THz Angular/Frequency Filters in the Modified Kretschmann–Raether Configuration With the Insertion of Single Layer Graphene

**Xiaoyu Dai**
**Leyong Jiang**
**Yuanjiang Xiang**

# Tunable THz Angular/Frequency Filters in the Modified Kretschmann–Raether Configuration With the Insertion of Single Layer Graphene

**Xiaoyu Dai, Leyong Jiang, and Yuanjiang Xiang**

SZU-NUS Collaborative Innovation Center for Optoelectronic Science and Technology, Key Laboratory of Optoelectronic Devices and Systems of Ministry of Education and Guangdong Province, College of Optoelectronic Engineering, Shenzhen University, Shenzhen 518060, China

**Abstract:** Tunable terahertz (THz) angular/frequency filters in the modified Kretschmann–Raether configuration with the insertion of single-layer graphene have been numerically demonstrated. Due to the excitation of the transverse magnetic (TM) polarized surface plasmons at the interface of two dielectrics with the insertion of the graphene sheet, the transmission resonance occurs at some range incident angles and frequencies in the THz frequency range, which can be adopted for designing the angular/frequency filters. It is shown that the resonant angle and the resonant wavelength can be tuned by varying the Fermi energy of the graphene sheets via electrostatic biasing. Moreover, we show that the resonant behaviors can be engineered by changing the gap thickness or the incident angle.

**Index Terms:** Optical filters, graphene, surface plasmons.

## 1. Introduction

Graphene is a 2-D material with the carbon structure only one atom thick, which has rich optical and electronic properties, including ultrahigh electron mobility, zero band-gap, and ultrafast relaxation time for photo-excited carriers. It has attracted enormous interest in recent decade [1], [2]. All kinds of novel photonic and optoelectronic applications have been presented, such as optical modulator [3], broadband polarizer [4], transformation optics [5], critically coupled resonance structure [6], and optical bistability [7]. More importantly, the conductivity properties of graphene can be tuned simply by adjusting the gate voltage, and this could provide an effective route to achieving electrical tunable plasmons [8], surface Bloch waves [9], and bandgap [10], etc.

It is well known that the graphene can support surface plasmon polaritons (SPPs) for both TE-and TM-modes, unlike the common metal only supporting the TM-polarized surface wave [11]–[13]. The versatile graphene SPPs have great application potential in plasmonic device. The combination of graphene with SPPs could result in fast, relatively cheap, and small active
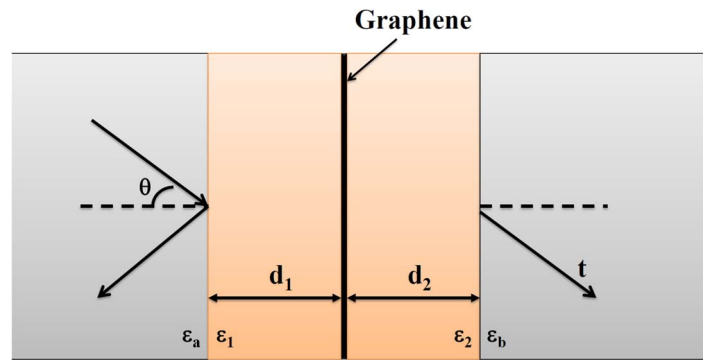
Fig. 1. Schematic of the modified Kretschmann–Raether (KR) configuration with the insertion of single layer graphene. The parameters are $T = 300$ K, $n_a = n_b = 3.84$, and $\varepsilon_1 = \varepsilon_2 = 1$.

optical elements and nanodevices. Because of this, the light absorption can be enhanced, and even the complete absorption with respect to the incident angle in the nano-disk array graphene structure can be obtained due to the collective effect of graphene SPPs [14], [15], the sensitivity of the biosensor can be boosted up dramatically by adding a few graphene layers onto the conventional gold-film SPR biosensor [16], and a combination of graphene with plasmonic nano-structures makes it possible to enhance the photovoltage by a factor of 15–20 without compromising the operational speed of a graphene photodetector [17], etc.

Traditional spatial (angular) filtering is an optical device which uses the principles of Fourier optics to alter the structure of a beam of coherent light or other electromagnetic radiation, which has been applied to image enhancement and information processing [18]–[20]. However, this spatial (angular) filtering system has several obvious deficiencies, such as relatively large size; high sensitivity to alignment; and the absence of efficient focusing lenses in THz, infrared, and ultraviolet frequencies [21]. To overcome these obstacles, a variety of new-type slab spatial (angular) filters have been proposed, which are based on the use of indefinite media [20], resonant-grating systems [22], [23], multilayer stacks combined with a prism [24], interference patterns [25], one-dimensional graded-index lattices with defects [26], and 2-D photonic crystals [21], [27], [28]. Besides, it is known that the active and tunable angular filtering is intrinsically important for the applications in the optical devices. However, very few methods have been put forward to make the angular filtering tunable. For instance, Rizza et al. theoretically considered the terahertz active angular filtering through optically tunable hyperbolic metamaterials [29].

In this paper, we find that the graphene SPPs can be utilized to realize the tunable THz angular/frequency filters. It is found that the angle/frequency-selected range and the width of the resonance angle/frequency can be electrically controlled by changing electrical or chemical modification of the charge carrier density of the graphene. Moreover, we also point out that the optical response of these angular/frequency filters depends on the gap width of the configuration. Therefore, electrical tunability of angular/frequency filtering from this simple multilayered structure could potentially open a new possibility of spatial spectrum analysis, matched filtering, radar data processing, biomedical applications, and other optical devices in information processing and image enhancement.

## 2. Model and Method

The Kretschmann–Raether (KR) geometry is employed here to match the wavevector of the incident light to that of the SPPs, however the metal in the KR configuration is replaced by the dielectric-graphene-dielectric heterostructure, hence we call it as modified KR configuration, as shown in Fig. 1. It is consisted by four-layer dielectrics, where dielectric A with permittivity $\varepsilon_a$ and dielectric B with permittivity $\varepsilon_b$ are two materials with high dielectric constants, and the dielectrics 1 ($\varepsilon_1$) and 2 ($\varepsilon_2$) with low dielectric constants are inserted between dielectrics A and B.

The thicknesses of dielectrics 1 and 2 are $d_1$ and $d_2$, respectively. The graphene sheets are sandwiched between dielectrics 1 and 2.

Without considering the external magnetic field and under the random-phase approximation, the isotropic surface conductivity $\sigma$ of graphene in the terahertz frequencies is dominated by the intraband transitions [30] $\sigma_{\text{intra}} = ie^2 E_F/[\pi\hbar^2(\omega + i/\tau)]$, where $\omega$ is the angular frequency of the incident light, $E_F$ is the Fermi energy, $\tau$ is the electron-phonon relaxation time, and e and $\hbar$ are the universal constants related to the electron charge and reduced Planck's constant, respectively. The Fermi energy $E_F = \hbar\nu_F(\pi n_{2D})^{1/2}$ can be electrically controlled by an applied gate voltage due to the strong dependence of the carrier density $n_{2D}$ on the gate voltage, where $\nu_F = 10^6$ m/s is the Fermi velocity of electrons. Obviously, $\sigma_{\text{intra}}$ is highly dependent on the work frequency and Fermi energy, which could provide an effective route to achieve an electrically controlled angular/frequency filtering phenomenon.

We use the modified transfer matrix method to calculate the transmission, reflection and absorption coefficients [31]. Different from the transmission matrix at the interface of the conventional materials, the transmission matrix at the interface of dielectric-graphene-dielectric should be modified as

$$D_{12} = \frac{1}{2}\begin{bmatrix} 1 + \xi_p + \varsigma_p & 1 - \xi_p - \varsigma_p \\ 1 - \xi_p + \varsigma_p & 1 + \xi_p - \varsigma_p \end{bmatrix} \tag{1}$$

for the TM-polarized, where $\xi_p = (\varepsilon_1/k_{1z})/(\varepsilon_1/k_{1z})/(\varepsilon_2/k_{2z})$; $\varsigma_p = \sigma k_{2z}/\varepsilon_0\varepsilon_2\omega$; $k_{1z} = k_0\sqrt{\varepsilon_1 - \varepsilon_a\sin^2\theta}$; $k_{2z} = k_0\sqrt{\varepsilon_2 - \varepsilon_a\sin^2\theta}$; $k_0 = \omega/c$; $\omega$ and $\theta$ are the angular frequency and incident angle of incident light, respectively; and $\epsilon_0$ is the permittivity in the vacuum. For the TE-polarized, the transmission matrix is

$$D_{12} = \frac{1}{2}\begin{bmatrix} 1 + \xi_s + \varsigma_s & 1 - \xi_s + \varsigma_s \\ 1 - \xi_s - \varsigma_s & 1 + \xi_s - \varsigma_s \end{bmatrix} \tag{2}$$

with the parameters $\xi_s = k_{2z}/k_{1z}$ and $\varsigma_p = \sigma\mu_0\omega/k_{1z}$, where $\mu_0$ is the permeability in the vacuum.

Since the transmission matrix is closely related to the properties of graphene sheet, it depends on the Fermi energy, and as a result, the transmission, reflection, and absorption of the modified KR configuration could be tuned by changing the Fermi energy of the graphene sheets. In the next numerical calculation, in order to simplify we assume that the refractive index of dielectrics A and B are equal ($n_a = n_b = 3.84$), and dielectrics 1 and 2 are vacuum ($\varepsilon_1 = \varepsilon_2 = 1$), hence the graphene sheet is suspended in the air and can be moved from left to right. In fact, we can use the dielectrics with high permittivity, such as, $SiO_2$, as the dielectrics 1 and 2 for electrically controlled tunability by the applied gate voltage on graphene.

## 3. Results and Discussions

It is well known that graphene can support both polarized surface plasmons at the interface of two dielectrics with graphene sheet covered between them [11]. Recently, gate-tuning of graphene plasmons and their applications for Terahertz to Mid-Infrared frequencies have been discussed and confirmed by experiments [32]–[34]. For TM polarization, since we know that SPPs occur only when the imaginary part of the conductivity is positive at the interface of two dielectrics, for TE polarization, SPPs occur only when the imaginary part of the conductivity is negative. Hence, SPPs cannot exist at the same frequency for both polarizations. In the THz frequencies range, the conductivity of graphene is dominated by the Drude contribution (intraband term), and in the present paper we only discuss the SPPs and angular/frequency filters for TM polarization. Except where otherwise stated, we have supposed that the losses in the graphene $\tau^{-1} = 1.0$ THz to simplify the discussion.

In the absence of the graphene sheet and hence lacking of SPPs in the KR configuration (see Fig. 1), there is only one dip in the angle-dependent reflectance, as shown in Fig. 2. Due to
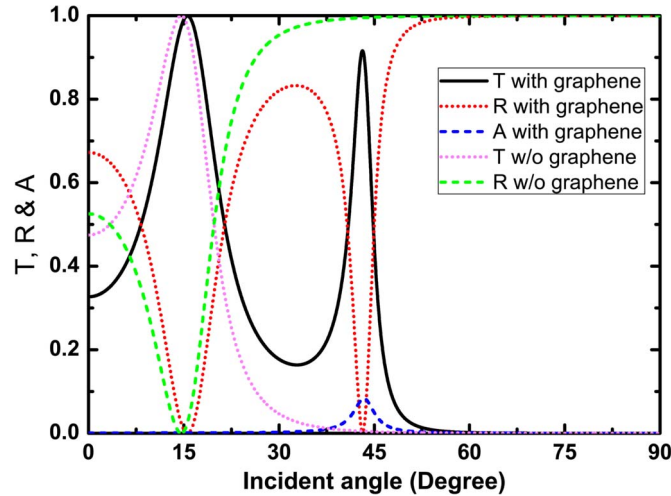
Fig. 2. Transmittance, reflectance, and absorption of this modified KR configuration as a function of incident angle. For comparison, transmittance and reflectance of the configuration without graphene sheet are also shown, where $n_a = n_b = 3.84$, $\varepsilon_1 = \varepsilon_2 = 1$, $d = d_1 = d_2 = 1.5$ $\mu$m, $E_F = 1.8$ eV, and $\lambda = 30$ $\mu$m ($f = 10$ THz).
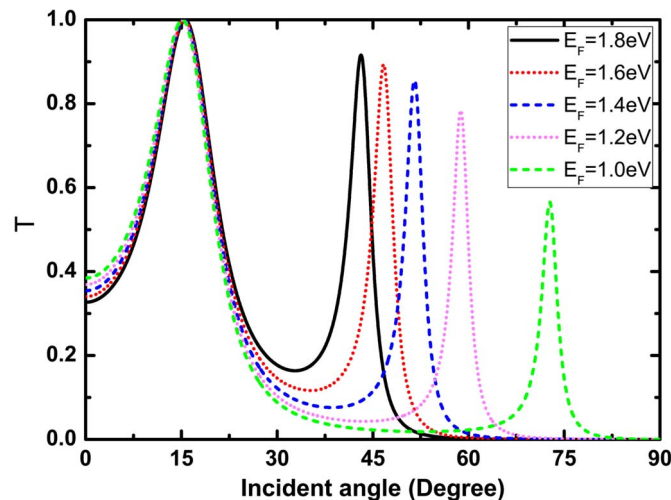


Fig. 3. Transmittance of the modified KR configuration as a function of incident angle at the different Fermi energy $E_F$, where $d = d_1 = d_2 = 1.5$ $\mu$m, and the other parameters have the same values as those in Fig. 2.

the neglect of the loss in the dielectrics, the transmittance reaches to the peak (100%), and so-called the Brewster angle ($\theta_B$) appears near $\theta = 14.6°$. Nevertheless, when the single-layer graphene is introduced into the gap, there is a second reflectance dip at the larger angle. This reflectance dip is deep and narrow, and it is excited by SPPs at the interface of the dielectric-graphene-dielectric. We find that the transmittance can reach to 100% in the absence of the loss in graphene sheet. However, the real part of graphene conductivity cannot be ignored, so that the transmittance cannot reach to 100% (90%), and the absorption has reached almost 10%. It is clear that this angle-dependent transmittance can be used to design the angular filters in the terahertz frequencies range.

Another advantage of our angular filtering is the tunable angle-selected range by changing the Fermi energy $E_F$, as shown in Fig. 3. When we decrease the Fermi energy $E_F$, the angle of the
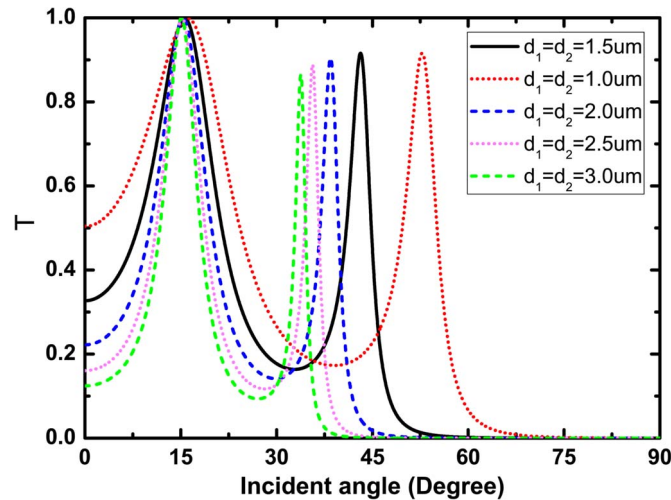
Fig. 4. Transmittance of the modified KR configuration as a function of incident angle at the different gap thicknesses, where $E_F = 1.8$ eV, $\lambda = 30$ $\mu$m, and the other parameters have the same values as those in Fig. 2.

first transmittance peak is nearly unmoved, which indicates that the introduction of the graphene sheet makes a very small impact on the transmittance near the Brewster angle; however, the second transmittance peak becomes smaller and smaller and the resonant angle moves to the larger angle side. For $E_F = 1.8$ eV, the angle of the second transmittance peak is $\theta = 43.15°$; however for $E_F = 1.0$ eV, the peak angle is $\theta = 72.74°$. This property suggests that the angle of the second transmittance peak can be engineered by the Fermi energy of the graphene sheets. Therefore, our modified KR structure with graphene has the potential to achieve tunable spatial filtering in a fixed configuration.

Besides the influence of the Fermi energy applied to graphene sheet on the resonant behavior, the peak angle and angle-selected range can also be engineered by changing the gap thicknesses ($d_1 = d_2 = d$). In Fig. 4, we have shown the dependence of the transmittance on the gap thicknesses. It is found that the increasing gap thicknesses shift the second transmittance peak to a smaller angle, and both transmittances become narrow, but decreasing gap thicknesses move the second transmittance peak to a larger angle, and both transmittances are broadened.

Next, we consider the frequency filters of the modified KR structure, as shown in Fig. 5. We only discuss the second transmittance peak, and let $\theta = 31.61°$. Obviously, this modified KR structure can support THz frequency filtering at some angle ranges due to the excitation of SPPs, and yet the frequency filtering phenomenon cannot occur if the graphene sheet is not considered where SPPs are not supported. Furthermore, the bandwidth of frequency filtering is widened and the full width at half maximum (FWHM) is about 2.5 $\mu$m (from 29 $\mu$m to 31.5 $\mu$m) for $d = 4$ $\mu$m. The peak frequency and frequency range of this frequency filtering can be tuned by changing the Fermi energy or the gap thickness, as shown in Fig. 5(a) and (b). As the gap thickness increases, the peak frequency shifts to a shorter wavelength, and the bandwidth becomes narrow and the reflectance dip get smaller and smaller. Therefore, our modified KR configuration structure with graphene also has the potential to achieve tunable frequency filtering only by controlling the gap between the upper and lower high-permittivity dielectrics.

In addition to the sensitivity of the gap thickness to the transmittance peak, we find that the reflectance and transmittance peak are also sensitive to the incident angle due to the dependence of the TM-polarized surface wave on the incident angle, as shown in Fig. 6(a) and (b). It is demonstrated that the increasing of the incident angles leads to the blueshift of the transmittance peak and the narrowing of the frequency filtering, and the decreasing of the incident angles bring about the redshift of the transmittance peak and the widening of the frequency filtering. Moreover, both the transmittance and reflectance peaks get increasingly smaller with
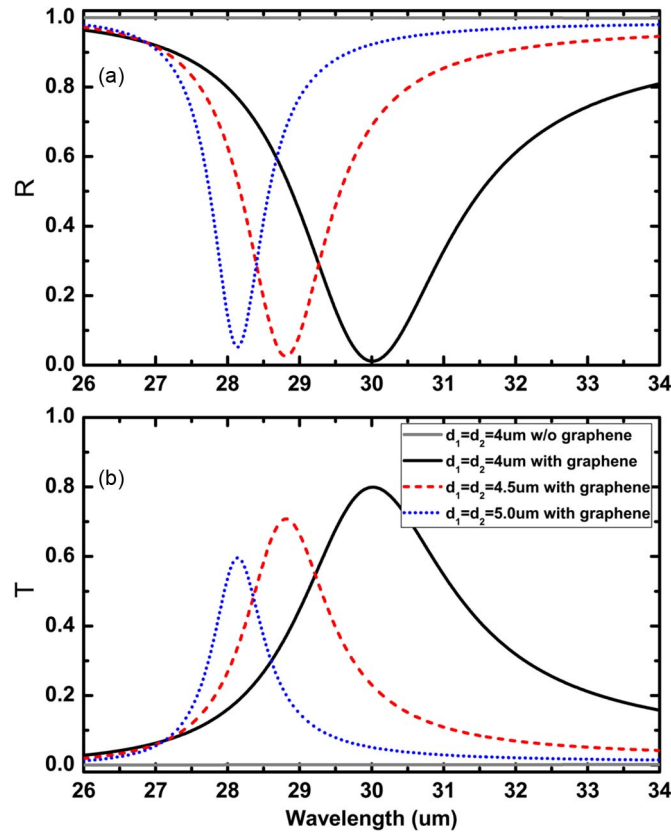
Fig. 5. (a) Reflectance and (b) transmittance of the modified KR configuration as a function of wavelength at the different gap thicknesses. For comparison, the transmittance and reflectance of the modified KR configuration without graphene sheet are also shown (thin solid line) in (a) and (b), where $\theta = 31.61°$, and the other parameters have the same values as those in Fig. 2.

the increased incident angle, which also implies that the absorption can be enhanced by optimizing the incident angle.

As we know, the contribution of interband optical transition give rise to the negative imaginary part of $\sigma_{inter}$, which supports the conditions for TE mode existence when graphene is not doped ($\hbar\omega/2 > |E_F|$) [35]. However, we find that there is no resonance point of the reflectance of TE-polarized wave, this behavior contrasts with the case of TM-polarized waves, where sharp SPP-related resonances occur. Hence, TE-polarized waves in graphene are not put forward to realize the tunable THz angular/frequency filters in our configuration. Moreover, it is found that the optical conductivity of graphene has the characteristic behavior of the magneto-optical effect, and the giant Faraday rotation in graphene has been identified [36], [37]. Magneto-optical conductivity of graphene is a function of magnetic field for various values of the chemical potential EF, hence it will have an effect on the transmission resonance, including the resonant angle and frequency. However, the main properties of tunable THz angular/frequency filters in our configuration do not change.

## 4. Conclusion

In conclusion, we have presented a graphene-based modified Kretschmann–Raether (KR) configuration as the basis to realize the angular/frequency filtering phenomenon in the terahertz frequency regime and discussed the controllable properties of this phenomenon. It is found that the angular/frequency filtering is dependent on the optical properties of graphene sheet and the gap thickness of the modified KR configuration, and the resonant angle/frequency and the
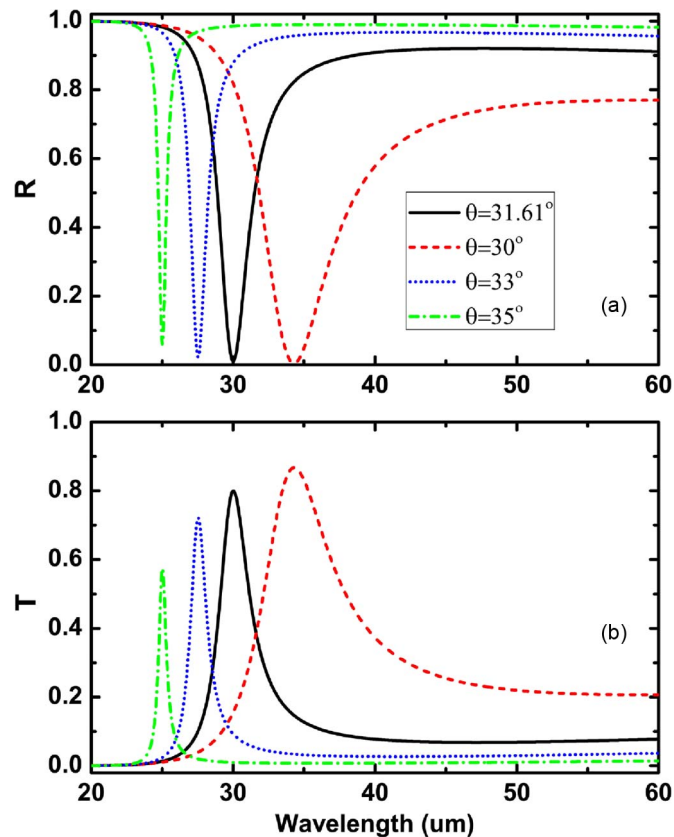
Fig. 6. (a) Reflectance and (b) transmittance of the modified KR configuration as a function of wavelength at the different incident angles, where $d = d_1 = d_2 = 4.0$ $\mu$m, and the other parameters have the same values as those in Fig. 2.

angle/frequency-selected range can be tuned by changing the Fermi energy applied on the graphene sheets. Moreover, we discuss the broadband frequency filtering behavior. We believe that the controllable angular and frequency filtering phenomenon at the terahertz frequencies could have potential applications in terahertz communications.

## References

[1] K. S. Novoselov *et al.*, "Electric field effect in atomically thin carbon films," *Science*, vol. 306, no. 5696, pp. 666–669, 2004.
[2] A. H. Castro Neto, F. Guinea, N. M. R. Peres, K. S. Novoselov, and A. K. Geim, "The electronic properties of graphene," *Rev. Mod. Phys.*, vol. 81, no. 1, pp. 109–162, 2009.
[3] M. Liu *et al.*, "A graphene-based broadband optical modulator," *Nature*, vol. 474, no. 7394, pp. 64–67, 2011.
[4] Q. Bao and K. P. Loh, "Graphene photonics, plasmonics, and broadband optoelectronic devices," *ACS Nano*, vol. 6, no. 5, pp. 3677–3694, 2012.
[5] A. Vakil and N. Engheta, "Transformation optics using graphene," *Science*, vol. 332, no. 6035, pp. 1291–1294, 2011.
[6] Y. Xiang *et al.*, "Critical coupling with graphene-based hyperbolic metamaterials," *Sci. Rep.*, vol. 4, no. 6, 2014, Art. ID. 5483.
[7] Y. Xiang, X. Dai, J. Guo, S. Wen, and D. Tang, "Tunable optical bistability at the graphene-covered nonlinear interface," *Appl. Phys. Lett.*, vol. 104, no. 5, 2014, Art. ID. 051108.
[8] J. Chen *et al.*, "Optical nano-imaging of gate-tunable graphene plasmons," *Nature*, vol. 487, no. 7405, pp. 77–81, 2012.
[9] Y. Xiang, J. Guo, X. Dai, S. Wen, and D. Tang, "Engineered surface Bloch waves in graphene-based hyperbolic metamaterials," *Opt. Exp.*, vol. 22, no. 3, pp. 3054–3061, 2014.
[10] C. H. Lui, Z. Li, K. F. Mak, E. Cappelluti, and T. F. Heinz, "Observation of an electrically tunable band gap in trilayer graphene," *Nature Phys.*, vol. 7, no. 12, pp. 944–947, 2011.
[11] Y. V. Bludov, A. Ferreira, N. M. R. Peres, and M. I. Vasilevskiy, "A primer on surface plasmon-polariton in graphene," *Int. J. Mod. Phys. B*, vol. 27, no. 10, 2013, Art. ID. 1341001.

[12] A. N. Grigorenko, M. Polini, and K. S. Novoselov, "Graphene plasmonics," *Nature Photon.*, vol. 6, no. 11, pp. 749–758, 2012.

[13] X. Luo, T. Qiu, W. Lu, and Z. Ni, "Plasmons in graphene: Recent progress and applications," *Mater. Sci. Eng. R*, vol. 74, no. 11, pp. 351–376, 2013.

[14] S. Thongrattanasiri, F. H. L. Koppens, and F. J. G. de Abajo, "Complete optical absorption in periodically patterned graphene," *Phys. Rev. Lett.*, vol. 108, no. 5, 2012, Art. ID. 047401.

[15] A. Y. Nikitin, F. Guinea, F. J. Garcia-Vidal, and L. Martin-Moreno, "Surface plasmon enhanced absorption and suppressed transmission in periodic arrays of graphene ribbons," *Phys. Rev. B*, vol. 85, no. 8, 2012, Art. ID. 081405.

[16] L. Wu, H. S. Chu, W. S. Koh, and E. P. Li, "Highly sensitive graphene biosensors based on surface plasmon resonance," *Opt. Exp.*, vol. 18, no. 14, pp. 14395–14400, 2010.

[17] T. Mueller, F. N. Xia, and P. Avouris, "Graphene photodetectors for high-speed optical communications," *Nature Photon.*, vol. 4, no. 5, pp. 297–301, 2010.

[18] J. W. Goodman, *Introduction to Fourier Optics*. New York, NY, USA: McGraw-Hill, 1968.

[19] S. P. Almeida and G. Indebetouw, *Applications of Optical Fourier Transforms*. Orlando, FL, USA: Academic, 1982.

[20] D. Schurig and D. R. Smith, "Spatial filtering using media with indefinite permittivity and permeability tensors," *Appl. Phys. Lett.*, vol. 82, no. 14, pp. 2215–2217, 2003.

[21] K. Staliunas and V. J. Snchez-Morcillo, "Spatial filtering of light by chirped photonic crystals," *Phys. Rev. A*, vol. 79, no. 5, 2009, Art. ID. 053807.

[22] R. Rabady and I. Avrutsky, "Experimental characterization of simultaneous spatial and spectral filtering by an optical resonant filter," *Opt. Lett.*, vol. 29, no. 6, pp. 605–607, 2004.

[23] A. Sentenac and A. L. Fehrembach, "Angular tolerant resonant grating filters under oblique incidence," *J. Opt. Soc. Amer. A*, vol. 22, no. 3, pp. 475–480, 2005.

[24] I. Moreno, J. J. Araiza, and M. Avendano-Alejo, "Thin-film spatial filters," *Opt. Lett.*, vol. 30, no. 8, pp. 914–916, 2005.

[25] L. Dettwiller and P. Chavel, "Optical spatial frequency filtering using interferences," *J. Opt. Soc. Amer. A*, vol. 1, no. 1, pp. 18–27, 1984.

[26] P. V. Usik, A. E. Serebryannickov, and E. Ozbay, "Spatial and spatial-frequency filtering using one-dimensional graded-index lattices with defects," *Opt. Commun.*, vol. 282, no. 23, pp. 4490–4496, 2009.

[27] A. E. Serebryannikov and T. Magath, "Transmission through photonic crystals with multiple line defects at oblique incidence," *J. Opt. Soc. Amer. B*, vol. 25, no. 3, pp. 286–296, 2008.

[28] A. E. Serebryannikov, A. Y. Petrov, and E. Ozbay, "Toward photonic crystal based spatial filters with wide angle ranges of total transmission," *Appl. Phys. Lett.*, vol. 94, no. 18, 2009, Art. ID. 181101.

[29] C. Rizza, A. Ciattoni, E. Spinozzi, and L. Columbo, "Terahertz active spatial filtering through optically tunable hyperbolic metamaterials," *Opt. Lett.*, vol. 37, no. 16. pp. 3345–3347, Aug. 2012.

[30] G. W. Hanson, "Dyadic Green's functions and guided surface waves for a surface conductivity model of graphene," *J. Appl. Phys.*, vol. 103, no. 6, 2008, Art. ID. 064302.

[31] T. Zhan, X. Shi, Y. Dai, X. Liu, and J. Zi, "Transfer matrix method for optics in graphene layers," *J. Phys., Condens. Matter*, vol. 25, no. 21, 2013, Art. ID. 215301.

[32] Z. Fei *et al.*, "Gate-tuning of graphene plasmons revealed by infrared nano-imaging," *Nature*, vol. 487, no. 7405, pp. 82–85, 2012.

[33] T. Low and P. Avouris, "Graphene plasmonics for terahertz to mid-infrared applications," *ACS Nano*, vol. 8, no. 2, pp. 1086–1101, 2014.

[34] H. Yan *et al.*, "Damping pathways of mid-infrared plasmons in graphene nanostructures," *Nature Photon.*, vol. 7, no. 5, pp. 394–399, 2013.

[35] Q. Bao *et al.*, "Broadband graphene polarizer," *Nature Photon.*, vol. 5, no. 7, pp. 411–415, 2011.

[36] H. Da *et al.*, "Monolayer graphene photonic metastructures: Giant Faraday rotation and nearly perfect transmission," *Phys. Rev. B*, vol. 88, no. 20, 2013, Art. ID. 205405.

[37] N. Ubrig *et al.*, "Fabry–Perot enhanced Faraday rotation in graphene," *Opt. Exp.*, vol. 21, no. 21, pp. 24 736–24 741, 2013.